Technical Note

Role of Roots of Orthogonal Polynomials in the Dynamic Response of Stochastic Systems

E. Jacquelin[1]; S. Adhikari[2]; M. I. Friswell[3]; and J.-J. Sinou[4]

Abstract: This paper investigates the fundamental nature of the polynomial chaos (PC) response of dynamic systems with uncertain parameters in the frequency domain. The eigenfrequencies of the extended matrix arising from a PC formulation govern the convergence of the dynamic response. It is shown that, in the particular case of uncertainties and with Hermite and Legendre polynomials, the PC eigenfrequencies are related to the roots of the underlying polynomials, which belong to the polynomial chaos set used to derive the polynomial chaos expansion. When Legendre polynomials are used, the PC eigenfrequencies remain in a bounded interval close to the deterministic eigenfrequencies because they are related to the roots of a Legendre polynomial. The higher the PC order, the higher the density of the PC eigenfrequencies close to the bounds of the interval, and this tends to smooth the frequency response quickly. In contrast, when Hermite polynomials are used, the PC eigenfrequencies spread from the deterministic eigenfrequencies (the highest roots of the Hermite polynomials tend to infinity when the order tends to infinity). Consequently, when the PC number increases, the smoothing effect becomes inefficient.
DOI: 10.1061/(ASCE)EM.1943-7889.0001102.

Author keywords: Random dynamical systems; Polynomial chaos expansion; Steady-state response; Convergence; Roots of orthogonal polynomials.

Introduction

The dynamic analysis of multiple-degree-of-freedom (DOF) linear systems with parametric uncertainties has received significant attention over the past decade. There are three main routes to solve this problem, namely (1) via a random modal analysis, (2) an integration of the coupled random equations of motion in the time domain, and (3) by directly solving the (complex) equations of motion in the frequency domain. For all three approaches, several reduced computational methods are available that avoid the use of expensive direct Monte Carlo simulations (Kundu and Adhikari 2014, 2015). Falsone and Impollonia (2002) proposed a modified perturbation method and Settineri and Falsone (2014) proposed the so-called approximated deformation principal modes (APDM)-based method to efficiently solve the uncertain static problem. The modified perturbation method has also been extended to uncertain dynamic systems (Falsone and Ferro 2005). Polynomial chaos expansion (PCE) (Ghanem and Spanos 1991) has been used extensively for all three approaches in the context of a dynamic system (Verhoosel et al. 2006; Ghanem and Ghosh 2007; Blatman and Sudret 2010). This paper focuses on the third approach, that is, the frequency domain solution of the dynamic response using PCE.

From an engineering point of view, the response near the resonance frequency is of paramount importance. The nature of the polynomial chaos (PC) response around the deterministic resonance frequency of a random dynamic system can be significantly different from any other points in the frequency axis. It was shown that inadequate polynomial orders lead to spurious peaks in the dynamic response around the deterministic resonance frequency. This was attributed to eigenfrequencies of the augmented system matrices that were obtained in conjunction with the PC expansion coefficients.

Up until now it has been normally considered that the computational cost and accuracy of a PC solution for a given problem depend mainly on the order of the polynomials. This in turn determines the number of terms in the PC expansion depending on the number of random variables. The nature of the polynomials on their own is not a contributing factor as long as the correct polynomials are chosen based on the underlying probability density function. However, for structural dynamic problems this may not always be the case. This paper aims to explain why the PCE convergence is faster with Legendre polynomials compared with Hermite polynomials when the stiffness matrix is random. The convergence rate is shown to depend on the nature of distribution of roots of such polynomials.

Response of a Random Dynamic System

Consider an n-DOF dynamic system described by its mass, damping, and stiffness matrices, $\mathbf{M}$, $\mathbf{D}$, and $\mathbf{K}$. The forces acting on this system are described by $\mathbf{F}(t)$, and $\mathbf{x}(t)$ denotes the response vector, which is the solution of

$$\mathbf{M}\ddot{\mathbf{x}}(t) + \mathbf{D}\dot{\mathbf{x}}(t) + \mathbf{K}\mathbf{x}(t) = \mathbf{F}(t) \quad (1)$$

The mass, damping, and stiffness matrices are assumed to be uncertain and given by

[1]Professor, Université de Lyon, F-69622 Lyon, France; Université Claude Bernard Lyon 1, 69100 Villeurbanne, France; Laboratoire de Biomécanique et Mécanique des Chocs (LBMC), Institut français des sciences et technologies des transports, de l'aménagement et des réseaux (IFSTTAR), Unité mixte de recherche (UMR)-T9406, F-69675 Bron, France (corresponding author). E-mail: eric.jacquelin@univ-lyon1.fr

[2]Professor, College of Engineering, Swansea Univ., Swansea SA2 8PP, U.K.

[3]Professor, College of Engineering, Swansea Univ., Swansea SA2 8PP, U.K.

[4]Professor, École Centrale de Lyon, Laboratoire de tribologie et systèmes dynamiques (LTDS), Unité mixte de recherche (UMR) Centre National de la Recherche Scientifique (CNRS) 5513, F-69134 Écully, France; Institut Universitaire de France, 75005 Paris, France.

Note. This manuscript was submitted on October 16, 2015; approved on February 10, 2016; published online on March 28, 2016. Discussion period open until August 28, 2016; separate discussions must be submitted for individual papers. This technical note is part of the ***Journal of Engineering Mechanics***, © ASCE, ISSN 0733-9399.

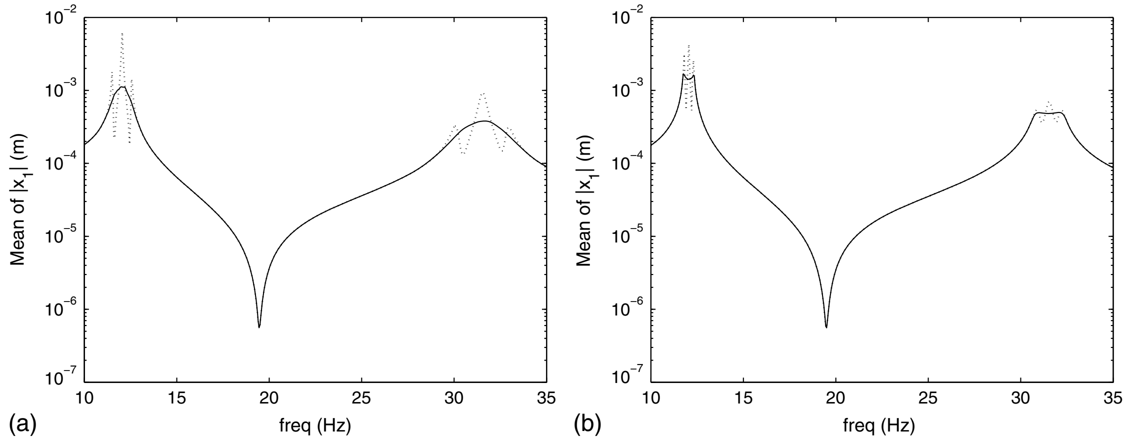

Fig. 1. Mean response with Monte Carlo simulations (solid line) and PCE of order 2 (dotted line): (a) Hermite; (b) Legendre

$$\mathbf{M} = \mathbf{M}(\Xi) = \sum_{i=0}^{r} \xi_i \mathbf{M}_i \tag{2}$$

$$\mathbf{D} = \mathbf{D}(\Xi) = \sum_{i=0}^{r} \xi_i \mathbf{D}_i \tag{3}$$

$$\mathbf{K} = \mathbf{K}(\Xi) = \sum_{i=0}^{r} \xi_i \mathbf{K}_i \tag{4}$$

where $\Xi = (\xi_1, \ldots, \xi_r)$ and $\xi_{i>0}$ = zero-mean random variable; and $\xi_0 = 1$ is not an uncertain variable.

The solution of Eq. (1) is random and may be expanded in terms of the PC basis $\{\Psi_j(\Xi): j \in \mathrm{IN}\}$ (Ghanem and Spanos 1991) as

$$\mathbf{x}(t,\Xi) = \sum_{j=0}^{\infty} \mathbf{Y}_j(t)\Psi_j(\Xi) \tag{5}$$

The elements of the PC basis are obtained from an orthogonal polynomial set $\{P_j(\xi): j \in \mathrm{IN}\}$, where j is the order of $P_j(\xi)$. Thus

$$\Psi_J(\Xi) = \prod_{i=1}^{r} P_{J_i}(\xi_i) \tag{6}$$

where $\sum_{i=1}^{r} J_i$ = order of Ψ_J. In the following, P_j is the Hermite (Legendre) polynomial, H_j (L_j), when ξ_i is a normally (uniform) distributed random variable. This choice is not obvious (Sepahvand et al. 2010), but it is optimal because Hermite (Legendre) polynomials are orthogonal with respect to the inner product corresponding to the probability density function for the normal (uniform) distribution (Eldred and Burkardt 2009).

For the numerical study, Eq. (5) can be truncated to a finite number of terms, $P+1$, which is given by $(m+r)!/(m!r!)$, where m is the chaos order. Truncating the infinite expansion gives the approximation of $\mathbf{x}(t,\Xi)$ as

$$\mathbf{x}^P(t,\Xi) = \sum_{j=0}^{P} \mathbf{Y}_j(t)\Psi_j(\Xi) \tag{7}$$

In the following, the exponent P is dropped for the sake of simplicity.

It is easy to show that the components of the PC expansion satisfy (Jacquelin et al. 2015b, a)

$$\tilde{\mathbf{M}}\,\ddot{\mathbf{Y}}(t) + \tilde{\mathbf{D}}\,\dot{\mathbf{Y}}(t) + \tilde{\mathbf{K}}\mathbf{Y}(t) = \tilde{\mathbf{F}}(t) \tag{8}$$

with

$$\mathbf{A}_k \in \mathbb{R}^{(P+1)\times(P+1)}, \quad \text{with } [A_k]_{IJ} = \langle k, I, J \rangle \tag{9}$$

$$\tilde{\mathbf{M}} = \sum_{k=0}^{r} \mathbf{A}_k \otimes \mathbf{M}_k \in \mathbb{R}^{2(P+1)\times 2(P+1)} \tag{10}$$

$$\tilde{\mathbf{D}} = \sum_{k=0}^{r} \mathbf{A}_k \otimes \mathbf{D}_k \in \mathbb{R}^{2(P+1)\times 2(P+1)} \tag{11}$$

$$\tilde{\mathbf{K}} = \sum_{k=0}^{r} \mathbf{A}_k \otimes \mathbf{K}_k \in \mathbb{R}^{2(P+1)\times 2(P+1)} \tag{12}$$

$$\mathbf{Y} = [\,\mathbf{Y}_0^T \quad \mathbf{Y}_1^T \quad \cdots \quad \mathbf{Y}_P^T\,]^T \in \mathbb{R}^{2(P+1)} \tag{13}$$

$$\tilde{\mathbf{F}}(t) = [\mathbf{F}^T(t)\,0\,0 \;\; \cdots \;\; 0]^T \in \mathbb{R}^{2(P+1)} \tag{14}$$

where $\otimes$ = Kronecker product; and $(\bullet)^T$ = transpose of $(\bullet)$.

Hence, the PC components are the solution of an $n(P+1)$-DOF dynamic system that will be referred to as the PC system. Thus the PCE has transformed the study of an uncertain dynamic system into the study of a deterministic dynamic system of larger order. The PC system has resonant frequencies that will be referred to as PC resonances. As a consequence, the moments of the steady-state response to a harmonic force derived through PCE show peaks related to these PC resonances. This is highlighted by Figs. 1 and 2, which show peaks around the deterministic eigenfrequencies with both Hermite [Figs. 1(a) and 2(a)] and Legendre [Figs. 1(b) and 2(b)] polynomials of order 2. This figure is related to the example described in the next section.

This result had been already derived for a dynamic system for Hermite polynomials (Jacquelin et al. 2015b, a; Sinou and Jacquelin 2015). Hence, the existence of such PC resonances has a strong influence on the convergence around the deterministic eigenfrequencies. However, Figs. 3 and 4 show that the convergence is almost reached for a PC order equal to 10 when Legendre polynomials are used [Figs. 3(b) and 4(b)], whereas the results are far from converged with Hermite polynomials [Figs. 3(a) and 4(a)].

Uncertain Stiffness Matrix

This section highlights some features related to the PC eigenfrequencies. To enable the calculation of closed-form exact results,

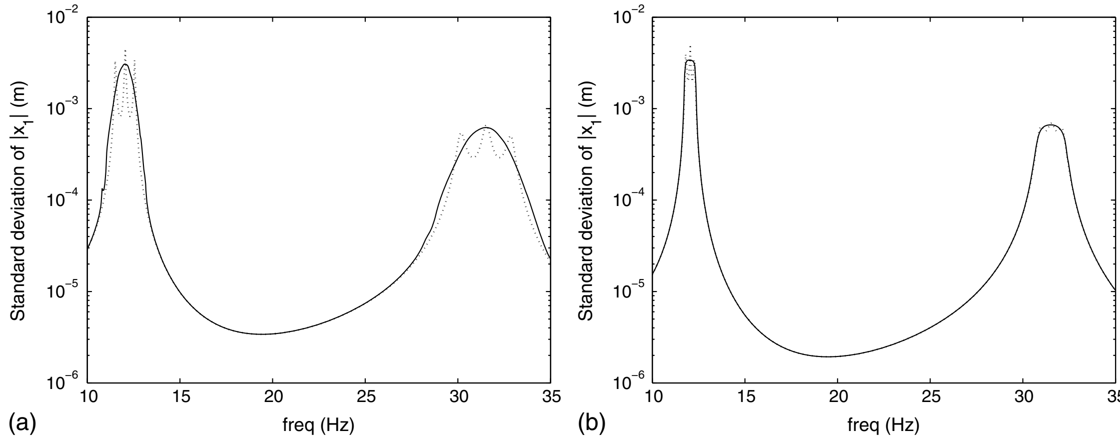

Fig. 2. Standard deviation of the response with Monte Carlo simulations (solid line) and PCE of order 2 (dotted line): (a) Hermite; (b) Legendre

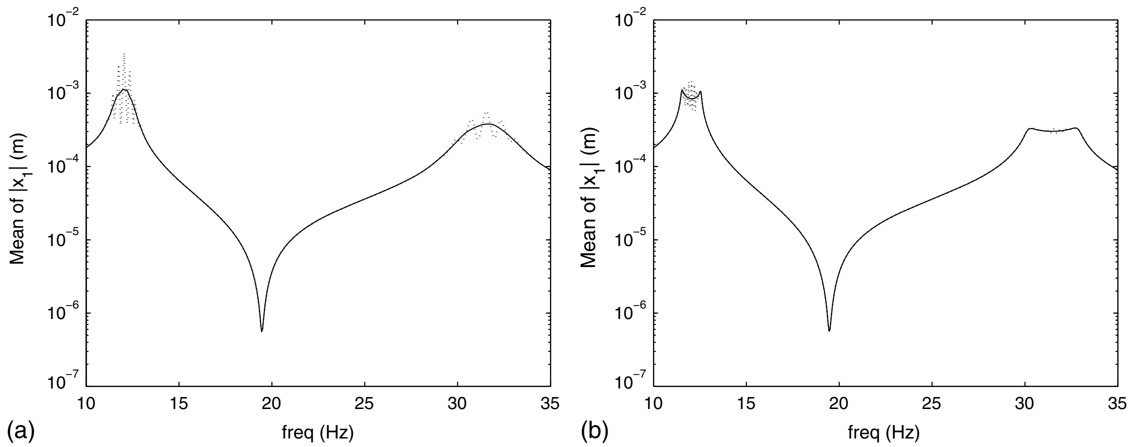

Fig. 3. Mean response with Monte Carlo simulations (solid line) and PCE of order 10 (dotted line): (a) Hermite; (b) Legendre

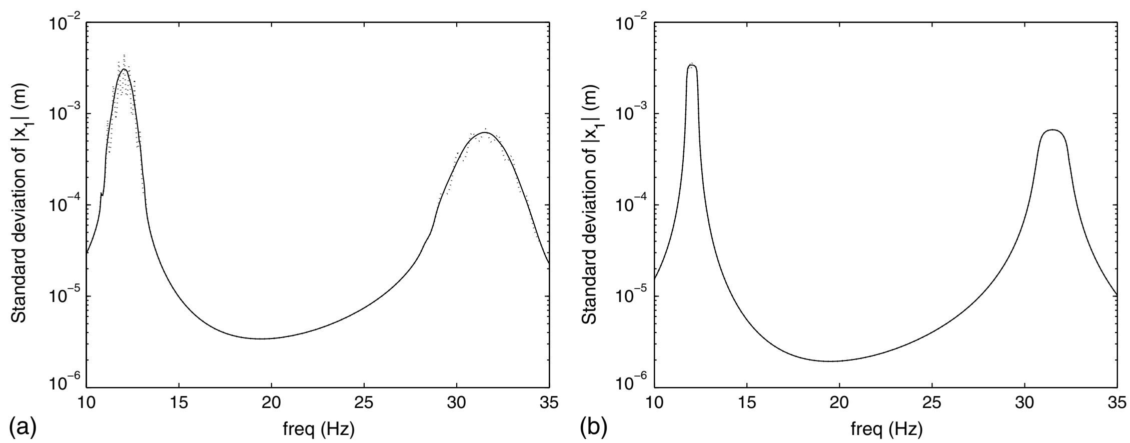

Fig. 4. Standard deviation of the response with Monte Carlo simulations (solid line) and PCE of order 10 (dotted line): (a) Hermite; (b) Legendre

the mass matrix is deterministic and the uncertain stiffness matrix is assumed to be given by

$$\mathbf{K} = \bar{\mathbf{K}}(1 + \delta_K \xi) \tag{15}$$

where ξ = standard normal or a uniform random variable; and $\bar{\mathbf{K}}$ = deterministic matrix, which represents the mean stiffness matrix. The covariance matrix of $\mathbf{K}$ is controlled by parameter δ_K and the deterministic dynamic system corresponds to $\delta_K = 0$. Comparing with Eq. (4) gives $\mathbf{K}_0 = \bar{\mathbf{K}}$ and $\mathbf{K}_1 = \delta_K \bar{\mathbf{K}}$.

The Appendix gives an extension proposed for uncertain mass and stiffness matrices.

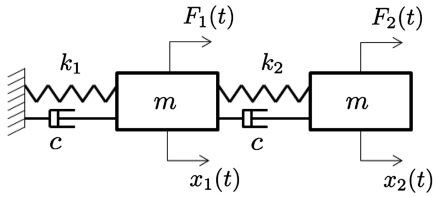

Fig. 5. Two-degree-of-freedom system with uncertain stiffnesses

Table 1. System Characteristics

Characteristics	Value
$\bar{k}$ (Nm^{-1})	1,500
m (kg)	1
c ($\mathrm{Nm}^{-1}\ \mathrm{s}^{-1}$)	1
σ_q (%)	5
F_{01} (N)	1
F_{02} (N)	0

Table 2. Modal Characteristics of the Deterministic System

Eigenfrequencies, f (Hz)	Modal damping ratio (%)
12.05	0.25
31.54	0.66

Description of the System

The numerical results (Figs. 1 and 3) are given for the example shown in Fig. 5, which represents a two-DOF dynamic system with one uncertain parameter, stiffness k, where

$$k = k_1 = k_2 = \bar{k}(1 + \delta_K \xi) \tag{16}$$

The force vector is assumed to be harmonic, i.e., $\mathbf{F}(t) = \mathbf{F_0} e^{i\omega t}$, and the steady-state response of the dynamic system is then $\mathbf{x}(t) = \mathbf{X} e^{i\omega t}$, where $i = \sqrt{-1}$. The PCE coefficients of $\mathbf{X}$ and $\mathbf{Y}$ satisfy

$$(-\omega^2 \tilde{\mathbf{M}} + i\omega \tilde{\mathbf{C}} + \tilde{\mathbf{K}})\mathbf{Y}(\omega) = \widetilde{\mathbf{F_0}} \tag{17}$$

The values of the physical parameters are given in Tables 1 and 2. The deterministic quantities correspond to $\delta_K = 0$.

PC Eigenvalues

The eigenproblem to solve is

$$(\tilde{\mathbf{K}}_0 + \tilde{\mathbf{K}}_1 - \tilde{\lambda}\tilde{\mathbf{M}})\tilde{\mathbf{V}} = \mathbf{0} \tag{18}$$

The eigenvalues are the solution of

$$|\tilde{\mathbf{M}}^{-1}(\tilde{\mathbf{K}}_0 + \tilde{\mathbf{K}}_1) - \tilde{\lambda}\mathbf{I}| = 0 \tag{19}$$

where $|\bullet|$ = determinant of a matrix. Thus

$$|(\mathbf{A}_0 \otimes \mathbf{M})^{-1}[(\mathbf{A}_0 + \delta_K \mathbf{A}_1) \otimes \bar{\mathbf{K}}] - \tilde{\lambda}\mathbf{I}| = 0 \tag{20}$$

The Kronecker product properties lead to the following problem

$$|\mathbf{A}_0^{-1}(\mathbf{A}_0 + \delta_K \mathbf{A}_1) \otimes (\mathbf{M}^{-1}\bar{\mathbf{K}}) - \tilde{\lambda}\mathbf{I}| = 0 \tag{21}$$

Then

$$|(\mathbf{I} + \delta_K \mathbf{A}_0^{-1}\mathbf{A}_1) \otimes (\mathbf{M}^{-1}\bar{\mathbf{K}}) - \tilde{\lambda}\mathbf{I}| = 0 \tag{22}$$

and hence $\{\tilde{\lambda}\}_k$ is a equal to $\{\lambda_i \times \omega_j^2\}_{(i,j)}$, where ω_j are the deterministic eigenfrequencies of the matrix pair $(\mathbf{K}, \mathbf{M})$, and λ_i are the eigenvalues of $(\mathbf{I} + \delta_K \mathbf{A}_0^{-1}\mathbf{A}_1)$. λ_i is a solution of the equation

$$|(\mathbf{I} + \delta_K \mathbf{A}_0^{-1}\mathbf{A}_1) - \lambda\mathbf{I}| = 0 \tag{23}$$

To simplify the problem, define $\alpha = (1 - \lambda)/\delta_K$. From Eq. (23), α satisfies

$$|\mathbf{A}_0^{-1}\mathbf{A}_1 + \alpha\mathbf{I}| = 0 \tag{24}$$

Case 1: Random Variables ξ Follow a Normal Distribution

Matrices $\mathbf{A}_0$ and $\mathbf{A}_1$ are defined by

$$\mathbf{A}_0 = \begin{bmatrix} 0! & 0 & \cdots & 0 \\ 0 & \ddots & \cdots & \vdots \\ \vdots & \ddots & \ddots & \vdots \\ 0 & \cdots & 0 & P! \end{bmatrix} \tag{25}$$

$$\mathbf{A}_1 = \begin{bmatrix} 0 & 1! & 0 & \cdots & 0 \\ 1! & 0 & 2! & \ddots & \vdots \\ 0 & \ddots & \ddots & \ddots & 0 \\ \vdots & \ddots & \ddots & \ddots & P! \\ 0 & \cdots & 0 & P! & 0 \end{bmatrix} \tag{26}$$

and hence

$$\mathbf{A}_0^{-1}\mathbf{A}_1 = \begin{bmatrix} 0 & 1 & 0 & \cdots & 0 \\ 1 & 0 & 2 & \ddots & \vdots \\ 0 & \ddots & \ddots & \ddots & 0 \\ \vdots & \ddots & \ddots & \ddots & P \\ 0 & \cdots & 0 & 1 & 0 \end{bmatrix} \tag{27}$$

Then the problem to be solved is to find α such that

$$\mathrm{DH}_{P+1}(\alpha) = \begin{vmatrix} \alpha & 1 & 0 & \cdots & 0 \\ 1 & \alpha & 2 & \ddots & \vdots \\ 0 & \ddots & \ddots & \ddots & 0 \\ \vdots & \ddots & \ddots & \ddots & P \\ 0 & \cdots & 0 & 1 & \alpha \end{vmatrix} = 0 \tag{28}$$

Developing this determinant with respect to the last line, the following recursive equation is derived for $P \geq 2$

J. Eng. Mech., 2016, 142(8): 06016004

$$DH_{P+1}(\alpha) = \alpha D_P(\alpha) - PD_{P-1}(\alpha) \quad (29)$$

with

$$DH_2(\alpha) = \alpha^2 - 1 \quad (30)$$

$$DH_1(\alpha) = \alpha \quad (31)$$

Hence $DH_{P+1}(\alpha)$ may be identified with $H_{P+1}(\alpha)$, the $(P+1)$ th Hermite polynomial, and the solutions to Eq. (28) are the roots of H_{P+1}.

Case 2: Random Variables ξ Follow a Uniform Distribution

Matrices $\mathbf{A}_0$ and $\mathbf{A}_1$ are defined by

$$\mathbf{A}_0 = \begin{bmatrix} 1 & 0 & \cdots & 0 \\ 0 & \ddots & \cdots & \vdots \\ \vdots & \ddots & \ddots & \vdots \\ 0 & \cdots & 0 & 1/(2P+1) \end{bmatrix} \quad (32)$$

$$\mathbf{A}_1 = \begin{bmatrix} 0 & 1/2 & 0 & \cdots & 0 \\ 1/3 & 0 & 2/15 & \ddots & \vdots \\ 0 & \ddots & \ddots & \ddots & 0 \\ \vdots & \ddots & \ddots & \ddots & P/[(2P-1)(2P+1)] \\ 0 & \cdots & 0 & P/[(2P-1)(2P+1)] & 0 \end{bmatrix} \quad (33)$$

Then the problem to be solved is to find α such that

$$DL_{P+1}(\alpha) = \begin{vmatrix} \alpha & 1/3 & 0 & \cdots & 0 \\ 1 & \alpha & 2/5 & \ddots & \vdots \\ 0 & \ddots & \ddots & \ddots & 0 \\ \vdots & \ddots & \ddots & \ddots & P/(2P+1) \\ 0 & \cdots & 0 & P/(2P-1) & \alpha \end{vmatrix} = 0 \quad (34)$$

Developing this determinant with respect to the last line, the following recursive equation is derived for $P \geq 2$

$$DL_{P+1}(\alpha) = \alpha DL_P(\alpha) - \frac{P}{2P-1}\frac{P}{2P+1}DL_{P-1}(\alpha) \quad (35)$$

with

$$DL_2(\alpha) = \alpha^2 - \frac{1}{3} \quad (36)$$

$$DL_1(\alpha) = \alpha \quad (37)$$

This recursive equation shows D_P belongs to a set of orthogonal polynomials. Further, it may be shown that DL_P is related to Legendre polynomial L_P by

$$DL_P(\alpha) = \frac{P!}{(2P-1)!!}L_P(\alpha) \quad (38)$$

Then the solutions of Eq. (34) are the roots of L_{P+1}.

Discussion

Jacquelin et al. (2015b) showed that the PCE coefficients given by Eq. (8) have PC resonances that correspond to the spurious peaks depicted on the response moments. The last result shows that the PC eigenfrequencies are equal to $\omega_i \times \sqrt{(1-\alpha_j\delta_K)}$, where the $\{\alpha_j\}$ for $0 \leq j \leq P$ are the roots of polynomials H_{P+1} or L_{P+1}, depending of the nature of the random variable. Because the roots of both Hermite and Legendre polynomials are symmetrical with respect to 0, PC eigenfrequencies are symmetrical about each deterministic eigenfrequency. Further, when P is even, $\alpha = 0$ is a root of H_{P+1} or L_{P+1}, and so, in this case, the deterministic eigenfrequencies are in the set of the PC eigenfrequencies.

To assess the dependence of the rate of convergence on the choice of polynomial type, Fig. 6 plots the mean response as a function of the order of the PCE. For a better comparison, the mean response is normalized so that the maximum is equal to unity and is obtained when the system is excited at 12.05 Hz, which is the first deterministic eigenfrequency; Figs 1 and 4 show that the convergence was the slowest at this frequency. Fig. 6 shows that the convergence is much quicker with the Legendre polynomials.

The difference between Hermite and Legendre polynomial chaos is that in the first case the PC eigenfrequencies spread from the deterministic eigenfrequencies, whereas in the second case the PC eigenfrequencies remain in a bounded interval close to the deterministic eigenfrequencies (Figs. 7 and 8). So in the latter case, the PC eigenmodes will quickly smooth the response due to their closeness (Fig. 9): in this case the PC eigenmodes cannot be assumed as separate and then superimposed.

PC Modal Response

According to Eq. (7), one has

$$\mathbf{x}(\omega, \Xi) = \sum_{i=0}^{P} \mathbf{Y}_i(\omega)\Psi_i(\Xi) \quad (39)$$

$\tilde{\mathbf{Y}}$ is the response of a PC dynamic system. Then, $\tilde{\mathbf{Y}}$ may be expanded on the PC eigenmodes as

$$\tilde{\mathbf{Y}}(\omega) = \sum_{j=0}^{n(P+1)} q_j(\omega)\tilde{\mathbf{V}}_j \quad (40)$$

where $\tilde{\mathbf{V}}_j$ = jth eigenvector of $(\tilde{\mathbf{K}}, \tilde{\mathbf{M}})$. Due to the definition of $\tilde{\mathbf{K}}$ and $\tilde{\mathbf{M}}$, $\tilde{\mathbf{V}}_j$ may be written as

J. Eng. Mech., 2016, 142(8): 06016004

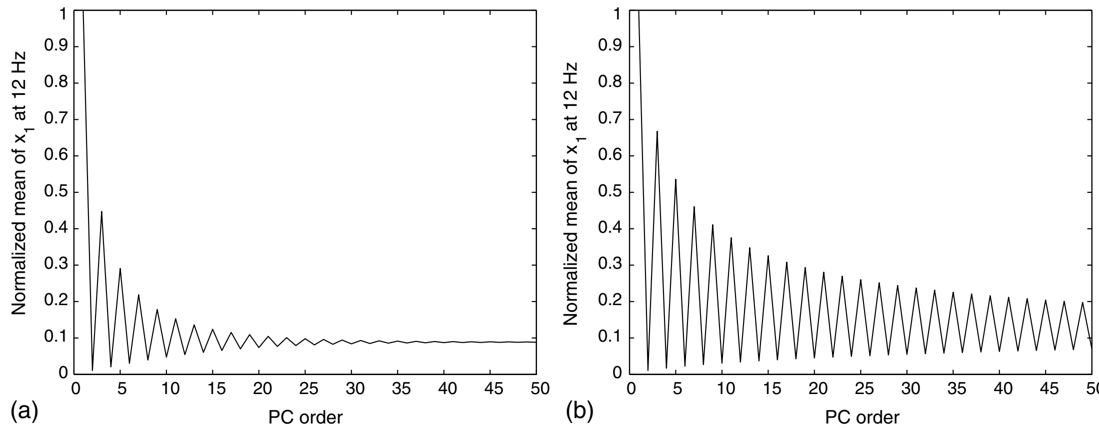

Fig. 6. Evolution of the normalized mean response obtained at the first eigenfrequency (12.05 Hz) as a function of the order of the PCE: (a) Legendre; (b) Hermite

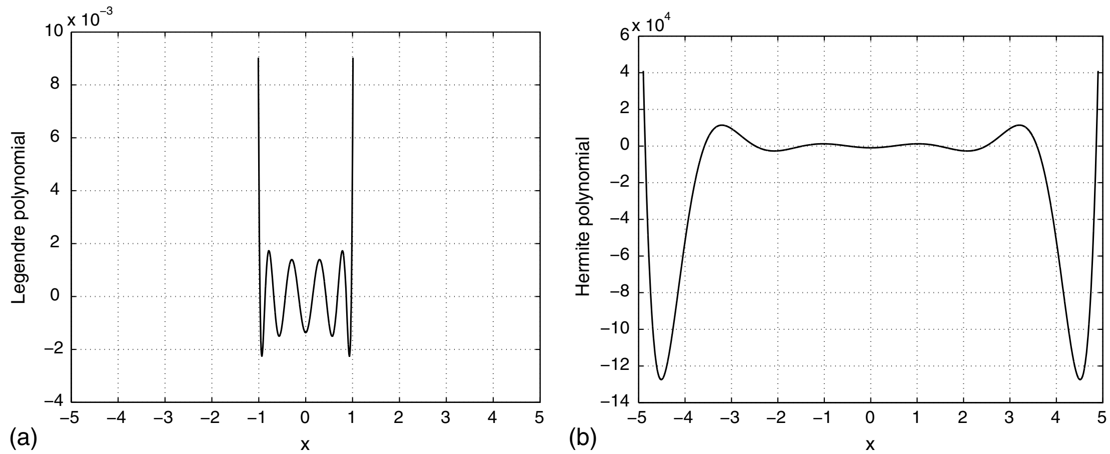

Fig. 7. Polynomial chaos of order 10: (a) Legendre; (b) Hermite

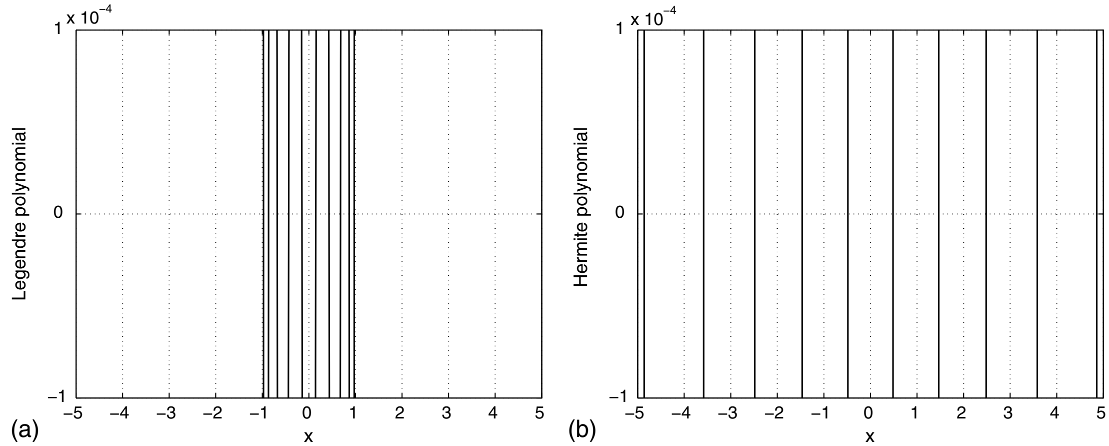

Fig. 8. Roots of polynomial chaos of order 10: (a) Legendre; (b) Hermite

$$\tilde{\mathbf{V}}_j = \mathbf{W}_k \otimes \mathbf{V}_m \tag{41}$$

where $\mathbf{W}_k$ ($\mathbf{V}_m$) = eigenvector of $[(\mathbf{A}_0 + \delta_K \mathbf{A}_1),\ \mathbf{A}_0]$ ($[\mathbf{K},\ \mathbf{M}]$); and $\tilde{\lambda}_j = \lambda_k \omega_m^2$. All of the modes are scaled with respect to the associated mass matrix.

Thus Eq. (40) may be rewritten as

$$\tilde{\mathbf{Y}}(\omega) = \sum_{m=1}^{n} \sum_{k=0}^{P} q_{km}(\omega) \mathbf{W}_k \otimes \mathbf{V}_m \tag{42}$$

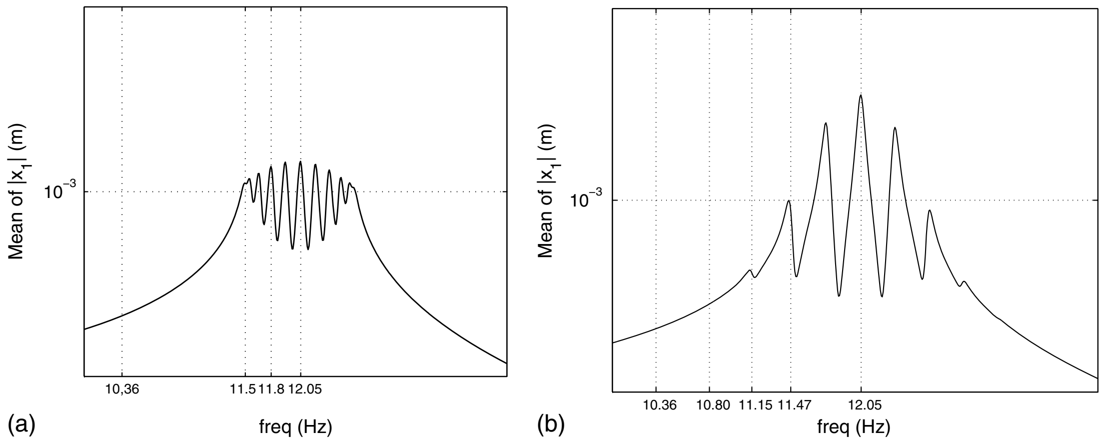

Fig. 9. Mean response close to the first eigenfrequency: (a) Legendre; (b) Hermite

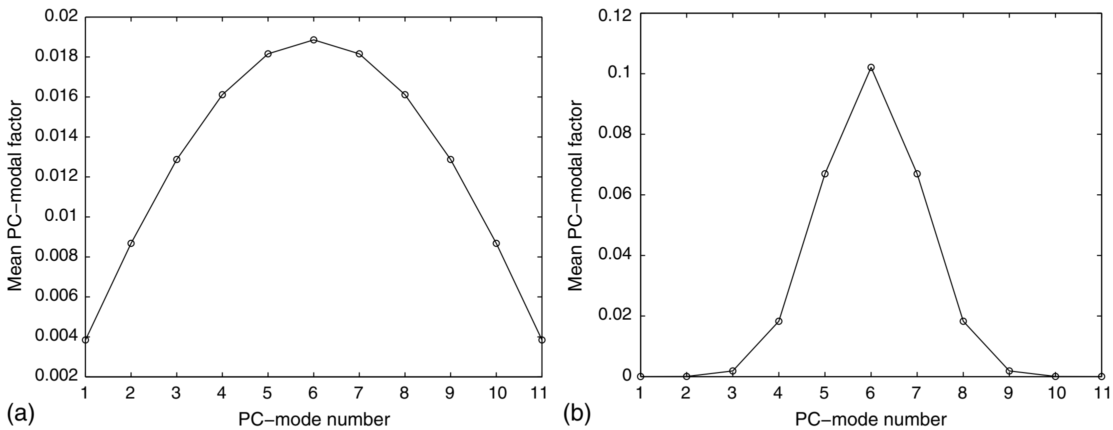

Fig. 10. Modal factors for $P = 10$: (a) Legendre; (b) Hermite

with

$$q_{km}(\omega) = \frac{(\mathbf{W}_k \otimes \mathbf{V}_m)^t \tilde{\mathbf{F}}}{\lambda_k \omega_m^2 - \omega^2 + 2i\tilde{\zeta}_{km}\omega\omega_m\sqrt{\lambda_k}} \quad (43)$$

Elements of $\tilde{\mathbf{F}}$ are all equal to zero except $\tilde{F}_f$, where f is the DOFs excited by $\mathbf{F}$ (in the example presented previously, $f = 1$). Hence

$$(\mathbf{W}_k \otimes \mathbf{V}_m)^t \tilde{\mathbf{F}} = W_{k,0} V_{m,f} \quad (44)$$

From Eq. (42), each subvector $\mathbf{Y}_i$ of $\tilde{\mathbf{Y}}$ is

$$\mathbf{Y}_i = \sum_{m=1}^{n} \left(\sum_{k=0}^{P} q_{km} W_{k,i} \right) \mathbf{V}_m \quad (45)$$

Finally the response is

$$\mathbf{x} = \sum_{m=1}^{n} \left[\sum_{i=0}^{P} \sum_{k=0}^{P} q_{km}(\omega) W_{k,i} \Psi_i(\Xi) \right] \mathbf{V}_m \quad (46)$$

$$= \sum_{m=1}^{n} \left[\sum_{i=0}^{P} \sum_{k=0}^{P} \frac{W_{k,0} W_{k,i} \Psi_i(\Xi)}{\lambda_k \omega_m^2 - \omega^2 + 2i\tilde{\zeta}_{km}\omega\omega_m\sqrt{\lambda_k}} \right] V_{m,f} \mathbf{V}_m \quad (47)$$

Then the modal factor of DOF r is

$$H_{km,r} = W_{k,0} \left[\sum_{i=0}^{P} W_{k,i} \Psi_i(\Xi) \right] V_{m,f} V_{m,r} \quad (48)$$

$H_{km,r}$ is then a random variable. The mean of this modal factor, $\bar{H}_{km,r}$, is also the modal factor of the mean of $\mathbf{x}$

$$\bar{H}_{km,r} = W_{k,0}^2 V_{m,f} V_{m,r} \quad (49)$$

The mean modal factors of DOF r are plotted in Fig. 10 for both the Legendre and Hermite cases. Because only the first 11 mean modal factors are plotted, they are all associated with the first deterministic eigenfrequency (indeed, $P = 10$). This shows that the Hermite case tends to weight more highly the PC modes around the deterministic eigenfrequency, which tends to diminish the smoothing effect due to the superimposed PC modes. Although this feature exists for the Legendre case, it is not as strong.

Conclusion

Dynamic response analysis in the frequency domain using PC expansion is considered in this paper. Particular attention is placed on the response statistics around the deterministic resonance frequencies, where the convergence of the PC solution is known

J. Eng. Mech., 2016, 142(8): 06016004

to be more erroneous than at other frequency values. The fundamental reason behind this phenomenon lies in the nature of the roots of the polynomials used for the PCE. The PC eigenfrequencies are related to the roots of the PC used to derive the expansion. In the case of Hermite polynomials, the PC eigenfrequencies spread from the deterministic eigenfrequencies, which leads to a slow convergence. In contrast, for Legendre polynomials the PC eigenfrequencies remain in a closed interval. Consequently, the PC eigenmodes are not separated and they are superimposed, which in turn leads to a smoothing effect and a quicker convergence. The theoretical idea proposed here can be extended to other polynomials, which would be necessary if the underlying probability density function of the random variables was different to that considered here.

Appendix. Uncertain Mass and Stiffness Matrices

To derive closed-form expressions, the uncertain mass and stiffness matrices are assumed to be of the form

$$\mathbf{M} = \bar{\mathbf{M}}(1 + \delta_M \xi) \tag{50}$$

$$\mathbf{K} = \bar{\mathbf{K}}(1 + \delta_K \xi) \tag{51}$$

where ξ = random variable.

The corresponding eigenproblem is then

$$[\tilde{\mathbf{K}}_0 + \tilde{\mathbf{K}}_1 - \tilde{\lambda}(\tilde{\mathbf{M}}_0 + \tilde{\mathbf{M}}_1)]\tilde{\mathbf{V}} = 0 \tag{52}$$

The eigenvalues are the solution of

$$|(\tilde{\mathbf{M}}_0 + \tilde{\mathbf{M}}_1)^{-1}(\tilde{\mathbf{K}}_0 + \tilde{\mathbf{K}}_1) - \tilde{\lambda}\mathbf{I}| = 0 \tag{53}$$

Thus

$$|[(\mathbf{A}_0 + \delta_M \mathbf{A}_1) \otimes \bar{\mathbf{M}}]^{-1}[(\mathbf{A}_0 + \delta_K \mathbf{A}_1) \otimes \bar{\mathbf{K}}] - \tilde{\lambda}\mathbf{I}| = 0 \tag{54}$$

The Kronecker product properties lead to the following problem:

$$|(\mathbf{A}_0 + \delta_M \mathbf{A}_1)^{-1}(\mathbf{A}_0 + \delta_K \mathbf{A}_1) \otimes (\bar{\mathbf{M}}^{-1}\bar{\mathbf{K}}) - \tilde{\lambda}\mathbf{I}| = 0 \tag{55}$$

δ_M is now assumed to be a very small parameter, so that the first order in δ_M

$$(\mathbf{A}_0 + \delta_M \mathbf{A}_1)^{-1} \simeq \mathbf{A}_0^{-1} - \delta_M \mathbf{A}_0^{-1}\mathbf{A}_1\mathbf{A}_0^{-1} \tag{56}$$

Then

$$(\mathbf{A}_0 + \delta_M \mathbf{A}_1)^{-1}(\mathbf{A}_0 + \delta_K \mathbf{A}_1) \simeq \mathbf{I} + (\delta_K - \delta_M)\mathbf{A}_0^{-1}\mathbf{A}_1 \tag{57}$$

and

$$|[\mathbf{I} + (\delta_K - \delta_M)\mathbf{A}_0^{-1}\mathbf{A}_1] \otimes (\bar{\mathbf{M}}^{-1}\bar{\mathbf{K}}) - \tilde{\lambda}\mathbf{I}| = 0 \tag{58}$$

Hence, the equivalent to Eq. (23) is obtained by replacing δ_K with $(\delta_K - \delta_M)$. As a consequence, the same conclusions can be drawn with uncertain mass and stiffness matrices provided δ_M is small enough to make Eq. (56) valid.

Acknowledgments

J.-J. Sinou acknowledges the support of the Institut Universitaire de France.

References

Blatman, G., and Sudret, B. (2010). "An adaptive algorithm to build up sparse polynomial chaos expansions for stochastic finite element analysis." *Probab. Eng. Mech.*, 25(2), 183–197.

Eldred, M. S., and Burkardt, J. (2009). "Comparison of non-intrusive polynomial chaos and stochastic collocation methods for uncertainty quantification." *47th AIAA Aerospace Sciences Meeting*, AIAA.

Falsone, G., and Ferro, G. (2005). "A method for the dynamical analysis of FE discretized uncertain structures in the frequency domain." *Comput. Methods Appl. Mech. Eng.*, 194(42–44), 4544–4564.

Falsone, G., and Impollonia, N. (2002). "A new approach for the stochastic analysis of finite element modelled structures with uncertain parameters." *Comput. Methods Appl. Mech. Eng.*, 191(44), 5067–5085.

Ghanem, R. G., and Ghosh, D. (2007). "Efficient characterization of the random eigenvalue problem in a polynomial chaos decomposition." *Int. J. Numer. Methods Eng.*, 72(4), 486–504.

Ghanem, R. G., and Spanos, P. D. (1991). *Stochastic finite elements: A spectral approach*, Springer, New York.

Jacquelin, E., Adhikari, S., Sinou, J.-J., and Friswell, M. (2015a). "Polynomial chaos expansion in structural dynamics: Accelerating the convergence of the first two statistical moment sequences." *J. Sound Vib.*, 356, 144–154.

Jacquelin, E., Adhikari, S., Sinou, J.-J., and Friswell, M. I. (2015b). "The polynomial chaos expansion and the steady-state response of a class of random dynamic systems." *J. Eng. Mech.*, 10.1061/(ASCE)EM.1943-7889.0000856, 04014145.

Kundu, A., and Adhikari, S. (2014). "Transient response of structural dynamic systems with parametric uncertainty." *J. Eng. Mech.*, 10.1061/(ASCE)EM.1943-7889.0000643, 315–331.

Kundu, A., and Adhikari, S. (2015). "Dynamic analysis of stochastic structural systems using frequency adaptive spectral functions." *Probab. Eng. Mech.*, 39(1), 23–38.

Sepahvand, K., Marburg, S., and Hardtke, H.-J. (2010). "Uncertainty quantification in stochastic systems using polynomial chaos expansion." *Int. J. Appl. Mech.*, 2(2), 305–353.

Settineri, D., and Falsone, G. (2014). "An APDM-based method for the analysis of systems with uncertainties." *Comput. Methods Appl. Mech. Eng.*, 278, 828–852.

Sinou, J.-J., and Jacquelin, E. (2015). "Influence of polynomial chaos expansion order on uncertain rotor system response." *Mech. Syst. Signal Process.*, 50–51, 718–731.

Verhoosel, C. V., Gutiérrez, M. A., and Hulshoff, S. J. (2006). "Iterative solution of the random eigenvalue problem with application to spectral stochastic finite element systems." *Int. J. Numer. Methods Eng.*, 68(4), 401–424.